



Deburring of micro-milled hardened steel: influence of milling strategies and CNC-based post-polishing

Armin Siah sarani¹ · Masih Paknejad¹ · Bahman Azarhoushang^{1,2}

Received: 25 June 2025 / Accepted: 1 November 2025
© The Author(s) 2025

Abstract

Hardened steels are extensively used in the automotive, aerospace, and medical industries due to their hardness and wear resistance and simultaneously high toughness. However, these properties present significant challenges in micro-milling, leading to rapid tool wear, poor surface quality, and substantial burr formation. Refining machining parameters, including cutting speed, feed rate, and milling strategies, is essential to enhance part quality and reduce post-processing efforts. This study first investigates machining parameters to minimize surface roughness and burr formation in micro milling of 60 HRC hardened steel, followed by the development of a CNC deburring method for the complete removal of burrs from edges. Experiments incorporated trochoidal micro milling for slot creation and roughing, followed by a detailed evaluation of cutting speed, feed per tooth, and milling strategies (down-milling vs. up-milling) during micro finishing. The results indicate that micro down milling at an optimal cutting speed of 80 m/min and a feed per tooth of 6 μm achieved the best surface quality ($S_a=0.85 \mu\text{m}$), which is approximately 50% lower than the surface roughness obtained from the initial trochoidal milling- while also minimizing burr formation. To further refine the process, a polyurethane-bonded SiC polishing tool was employed in the same CNC center immediately after micro milling, completing the deburring process via top micro polishing. This optimized approach enhances production efficiency and sustainability in machining hardened steel, offering a viable solution for high-precision applications.

Keywords Micro milling · Micro polishing · Deburring · Hardened steel

1 Introduction

Micro milling has emerged as a critical method for manufacturing micro components with high precision and complex geometries, particularly in the production of molds and dies used in the medical, automotive, and aerospace industries [1–3]. This process enables the fabrication of intricate features with precise tolerances. However, the micro milling process encounters significant challenges when machining hardened steels like AISI D2 (DIN 1.2379) [4]. While these steels offer exceptional hardness, wear resistance, and proper toughness making them essential for applications

subjected to high mechanical and thermal stresses, their properties pose difficulties for machinability, particularly at the micro scale, where intricate dynamics come into play [5–7].

A key challenge in micro milling hardened steels lies in the interplay between material properties and scale effects. When the undeformed chip thickness becomes comparable to the cutting-edge radius, ploughing dominates over shearing, leading to increased cutting forces, degraded surface finish, and accelerated tool wear [7–10]. Balázs and Takács showed the critical role of tool geometry and material properties in influencing cutting forces, emphasizing that increasing the feed per tooth reduces ploughing while improving surface quality, although this comes at the cost of increased tool stress and wear [11]. Additional experimental results also indicate that achieving a balance between feed per tooth and cutting speed is essential for optimizing machining performance and reducing size-effect-induced inefficiencies [12–14].

✉ Bahman Azarhoushang
bahman.azarhoushang@tf-pr.uni-freiburg.de

¹ Institute for Advanced Manufacturing (KSF), Furtwangen University, Furtwangen, Germany

² Department of Microsystems Engineering (IMTEK), University of Freiburg, Freiburg, Germany

In addition to these material removal challenges, burr formation is a persistent issue in the micro milling of hardened steels [15]. Burrs not only compromise dimensional accuracy and surface quality but also necessitate additional post-processing steps, which increase production costs. Researchers have shown that burr formation is highly sensitive to machining parameters, including feed rate, cutting speed, and milling strategies. For example, Sun et al. demonstrated that burr widths could be reduced significantly by fine-tuning radial and axial depths of cut, particularly for ductile materials like stainless steel [16]. Furthermore, Gomes et al. explored the role of tool rigidity and cutting length on burr formation and surface quality, investigating the impact of tool design and machining conditions [17].

Deburring is an essential step in the micro milling process. While burr formation depends on machining parameters and tool design, its removal is crucial for maintaining the functionality and quality of precision components. Traditional manual deburring methods are labor-intensive, time-consuming, and inconsistent, making them unsuitable for modern manufacturing. CNC deburring systems in machining centers can provide a consistent and efficient solution, improving productivity and reducing manual intervention. When applied directly after micro-milling, flexible abrasive polishing tools can effectively remove burrs and edge residues without damaging the surrounding surface. This method enables simultaneous surface smoothing and controlled edge rounding, thereby eliminating the need for separate manual or mechanical deburring stages [10, 18, 19]. Recent developments, such as polyurethane-based flexible abrasive tools introduced by Cho et al. [20], have demonstrated excellent adaptability to complex geometries, minimizing surface irregularities while maintaining dimensional accuracy. Brinksmeier et al. [21] further emphasized the potential of abrasive polishing tools, particularly pin-type and wheel-type configurations, for precision finishing of structured surfaces, showing that parameters such as contact pressure and relative velocity strongly influence material removal and final surface roughness.

Furthermore, the micro milling process is highly sensitive to tool deflection and run-out, which are amplified at smaller scales. Tool deflection, caused by the high forces acting on a micro tool, can distort the intended geometry of the part. Similarly, tool run-out can cause uneven cutting and lead to premature tool failure. These issues demand precise control of machining parameters, such as cutting speed, feed rate, and depth of cut, as well as optimized tool design to mitigate adverse effects [22, 23].

This study investigates the micro milling of hardened steel with a hardness of 60 HRC, addressing key challenges in the process. Utilizing ceramic-coated carbide micro milling tools and advanced strategies, such as trochoidal milling

for initial slot creation, the study examines the impact of cutting speeds, feed per tooth values, and milling strategies on burr formation and surface quality during micro side finishing. Additionally, an innovative CNC deburring approach, using a polyurethane-bonded SiC polishing tool, is used directly after micro milling to improve machining quality and efficiency. In contrast to conventional multi-step deburring or hybrid finishing methods, the present work introduces a CNC-based post-polishing process integrated within the same machining center, enabling fully automated in-situ deburring immediately after micro-milling. The novelty of this study lies in this process integration and optimization of cutting and polishing parameters to achieve burr-free edges and superior surface quality in hardened steel components while maintaining high process efficiency.

2 Materials and methods

In this study, AISI D2 (DIN 1.2379) hardened steel with a hardness of 60 HRC was selected as the workpiece material. AISI D2, a high-carbon, high-chromium tool steel presents significant challenges in machining due to its hardness and abrasion-resistant properties. The experiments were conducted on a 5-axis GF Mikron MILL S 400 U machining center, with the machining setup and workpiece arrangement illustrated in Fig. 1. Initial slots with dimensions of 5 mm in length, 1.2 mm in width, and 1 mm in depth were created using a trochoidal milling strategy, chosen for its ability to minimize heat generation and tool wear while maintaining stable cutting conditions [24, 25]. A ceramic-coated carbide tool with a diameter of 0.8 mm and two cutting edges was utilized for this operation. The objective of this study was to produce a 1 mm-deep slot while investigating the effect of different axial depths of cut (0.025 mm, 0.1 mm, and 1 mm) on the trochoidal milling process to identify optimal conditions for slot formation. These specific depth values were selected from preliminary trials to represent low, medium, and high material removal scenarios, respectively, thereby enabling a precise evaluation of their influence on surface integrity and machining time.

Following the roughing process and initial slot creation, micro side milling was implemented to enhance surface quality and reduce burr formation in the side surfaces of slots. This step was performed using a new carbide tool with the same coating, but with four cutting edges to improve finishing efficiency. To achieve the desired surface quality within the slot and minimize burr formation at the edges, cutting speeds of 50, 80, and 100 m/min, feed per tooth values of 2, 4, 6, and 8 $\mu\text{m}/\text{tooth}$, and milling strategies (down and up milling) were tested, as detailed in Table 1. Regarding the selection of cutting parameters, the tested ranges of

Fig. 1 (a) Experimental setup for conducting micro milling and polishing tests, and (b) overview of micro milling, and polishing procedures

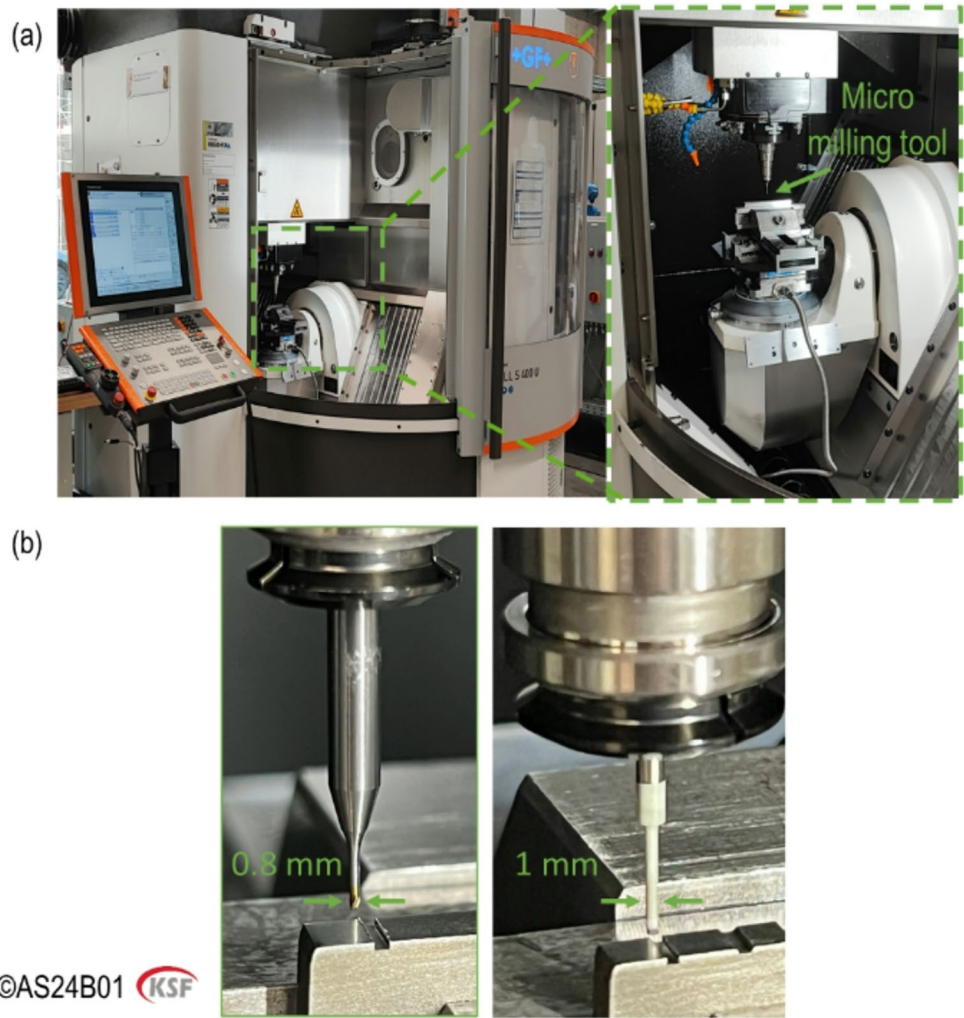


Table 1 Experimental micro milling parameters and conditions

WP Material	Machine Process	Tool	Slot Dimension [mm]	a_p [mm]	a_e [μm]	Direction	v_c [m/min]	f_2 [$\mu\text{m}/\text{tooth}$]
hardened steel AISI D2 (DIN 1.2379) hardness = 60 HRC	micro trochoidal milling	ceramic-coated carbide micro milling tools ($\varnothing 0.08\text{mm}$) cutting edges: 2&4	L5*W1.2*T1	0.025	25	up milling	40	6
				0.01				
	micro side milling			1	10	up milling	50	6
				1			80	
							100	2
							80	4
				down milling			6	
							8	
							6	
							6	

cutting speed and feed per tooth were determined based on a combination of prior literature on micro-milling of hardened steels, tool manufacturer recommendations, and preliminary experimental trials conducted to ensure stable cutting

without tool breakage. These conditions were selected to cover the practical operating window for the tool geometry and material used, allowing evaluation of their influence on surface roughness and burr formation.

Since side milling alone could not fully remove burrs, a top polishing operation was performed immediately after milling within the same CNC machining center. This polishing process utilized a polyurethane-bonded silicon carbide (SiC) polishing mounted pins with a diameter of 1 mm at a cutting speed of 50 m/min with a feed rate of 100 mm/min. Various axial depths of cut were explored during polishing to ensure the complete removal of residual burrs while preserving the integrity of the machined features.

Burr investigation was conducted using an optical microscope (KEYENCE, VHX 7000) with a maximum magnification of 2500X. Additionally, surface topography and roughness were analyzed using a confocal microscope (μ surf from NanoFocus) to assess the quality of the machined slots and evaluate the effectiveness of the finishing processes. The forces were recorded using a Kistler 9256C1 three-component piezoelectric dynamometer mounted under the workpiece, with signals acquired through a Kistler 5070 A charge amplifier and processed via DynoWare software. The maximum milling forces components, as captured by Kistler dynamometer, were analyzed and denoised using MATLAB software. Subsequently, the average of maximum forces and their standard deviations were derived.

3 Results and discussion

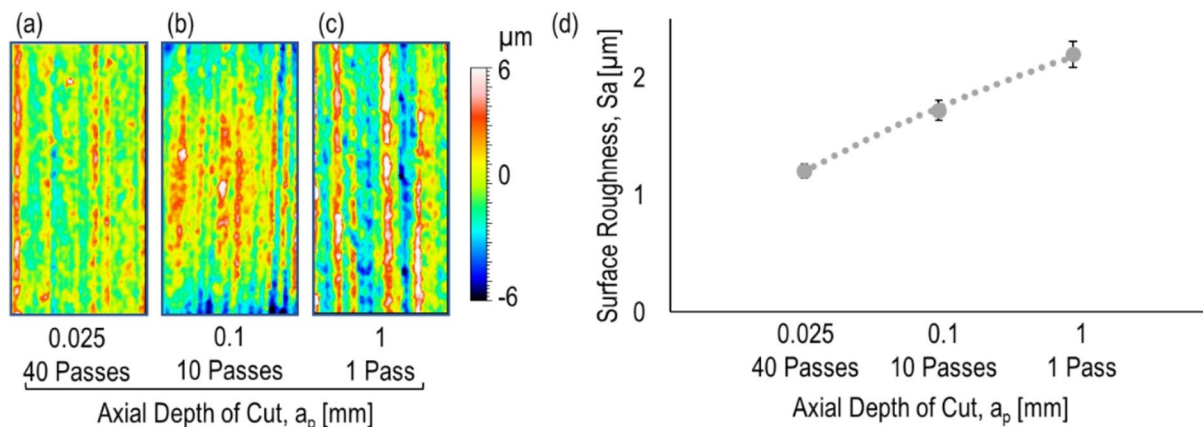
3.1 Trochoidal slot micro milling

The trochoidal milling strategy was employed for the initial slot creation, with the objective of achieving a slot depth of 1 mm while evaluating three different axial depths of cut (a_p): 0.025 mm (40 passes), 0.1 mm (10 passes), and 1 mm (single pass). To ensure consistency across trials, key machining parameters, including feed per tooth, cutting speed, and tool geometry, were maintained constant, as determined from preliminary investigations. The radial depth of cut (a_e) was set to 25 μ m, the feed per tooth (f_z) to 6 μ m, and the cutting speed (v_c) to 40 m/min.

The confocal images presented in Fig. 2(a) reveal that the surface generated with an a_p of 0.025 mm exhibits significantly improved smoothness compared to the other conditions. In contrast, the surface produced with an a_p of 1 mm is characterized by pronounced irregularities, including peaks and valleys, indicative of inferior surface quality. The intermediate condition, a_p of 0.1 mm, results in a moderately irregular surface morphology. These findings are further confirmed by the areal surface roughness parameter (S_a) in Fig. 2(b), where the surface generated with $a_p = 0.025$ mm resulted the lowest roughness value ($S_a = 1.2$ μ m), followed by 1.72 μ m for $a_p = 0.1$ mm, and 2.2 μ m for $a_p = 1$ mm.

The improved surface quality observed at lower a_p values can be attributed to the reduced tool engagement and lower cutting forces per pass, which mitigate plastic deformation

Process	Micro trochoidal milling
Tool	Ceramic-coated carbide micro milling tool, \varnothing 0.8 mm, 2 cutting edges
Workpiece	Hardened steel (AISI D2), hardness = 60HRC
Parameters	Trochoidal milling: $a_e = 0.025$ mm, $a_p = 0.025$ (40 times), 0.1 (10 times), 1 mm, $f_z = 6$ μ m/tooth, $v_c = 40$ m/min
Coolant	Emulsion



©AS24B02 (KSF)

Fig. 2 Confocal microscopy images of the initial trochoidal micro-milled surfaces at depths of cut of 0.025, 0.1, and 1 mm ((a–c)) and corresponding surface roughness parameter (S_a) (d) as a function of depth of cut in micro-milling

and tool deflection effects. Conversely, at higher a_p values (e.g., 1 mm), the increased material removal rate results in elevated cutting forces, greater tool deflection, and machining instability, ultimately leading to poorer surface integrity.

The machining time required to create a slot with dimensions of $5 \times 1.2 \times 1$ mm using trochoidal micro-milling was evaluated at varying axial depths of cut. For an axial depth of cut (a_p) of 0.025 mm, the machining time was approximately 76 min, necessitating 40 passes to reach the target depth. In contrast, increasing a_p to 0.1 mm reduced the number of passes to 10, consequently lowering the machining time to 7.6 min. The shortest machining time of 1.9 min was achieved with an a_p of 1 mm, which required only a single pass.

Although the smallest a_p (0.025 mm) leads to the highest surface quality, the associated excessive machining time makes it impractical for efficient material removal. Given that this phase is primarily intended for roughing, with surface quality being further enhanced in the subsequent finishing stage, an a_p of 0.1 mm was selected for the remainder of the experiments as a compromise between surface integrity, tool wear and machining efficiency.

3.2 Side milling

3.2.1 Surface quality

Figure 3 presents confocal images of the micro side-milled surface along with the corresponding Sa for various f_z values. All tests were conducted with $a_c = 10 \mu\text{m}$, $a_p = 1$ mm, $v_c = 80$ m/min and up milling strategy. Among the tested

values, the best surface quality is achieved at $f_z = 6 \mu\text{m/tooth}$, with Sa of $1.05 \mu\text{m}$. The confocal images in Fig. 3(a) for this condition reveal fewer and less pronounced peaks and valleys, indicating a more uniform surface.

At lower feed per tooth values, such as $f_z = 2 \mu\text{m/tooth}$, surface quality deteriorates, yielding the highest Sa value of $1.78 \mu\text{m}$. This decline is attributed to the tool's cutting-edge radius ($4 \mu\text{m}$) being larger than the feed per tooth, causing a transition from shearing to ploughing, increasing material deformation, and degrading the surface finish. For $f_z = 8 \mu\text{m/tooth}$, the Sa value increases slightly to $1.23 \mu\text{m}$, as higher feeds introduce vibrations that lead to a decline in surface quality. The intermediate result at $f_z = 4 \mu\text{m/tooth}$, with Sa value of $1.29 \mu\text{m}$, represents a transition between suboptimal and optimal cutting condition.

In summary, for micro side milling with the used tool in this study, an f_z of $6 \mu\text{m/tooth}$ optimally balances efficient material removal and high surface quality. Deviating from this condition results in increased surface roughness due to transitions in cutting mechanics or instability during the milling process.

Figure 4(a, b) presents confocal images of micro side-milled surfaces along with the corresponding Sa values for various v_c values in up and down milling, respectively. All tests were conducted with $a_c = 0.01$ mm, $a_p = 1$ mm, and $f_z = 6 \mu\text{m/tooth}$. The results indicate that down milling consistently produces better surface quality than up milling across all cutting speeds. Confocal images confirm that surfaces generated by down milling exhibit lower peaks and valleys, corresponding to 15–20% lower Sa values compared to up milling at identical cutting speeds.

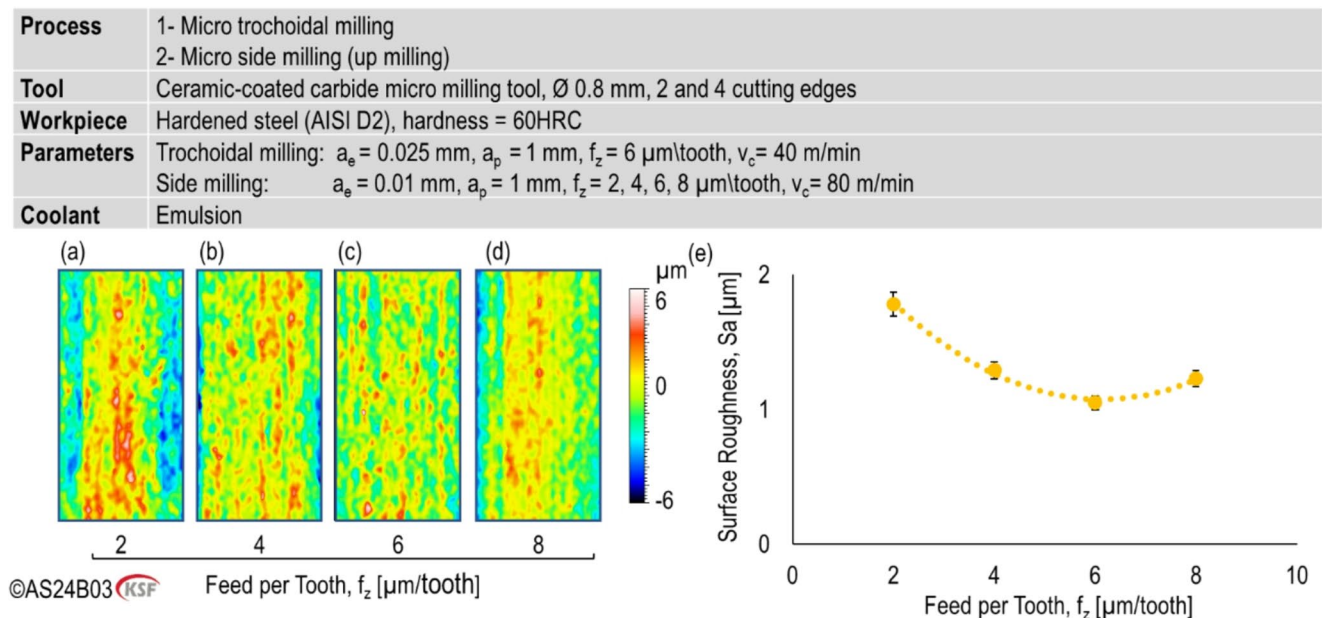


Fig. 3 Confocal microscopy images of micro side-milled surfaces at feed per tooth values of 2, 4, 6, and 8 $\mu\text{m/tooth}$ ((a–d)) and corresponding surface roughness parameter (Sa) (e) as a function of feed per tooth in micro-milling

Process	1- Micro trochoidal milling 2- Micro side milling (up and down milling)
Tool	Ceramic-coated carbide micro milling tool, Ø 0.8 mm, 2 and 4 cutting edges
Workpiece	Hardened steel (AISI D2), hardness = 60HRC
Parameters	Trochoidal milling: $a_e = 0.025$ mm, $a_p = 1$ mm, $f_z = 6$ $\mu\text{m/tooth}$, $v_c = 40$ m/min Side milling: $a_e = 0.01$ mm, $a_p = 1$ mm, $f_z = 6$ $\mu\text{m/tooth}$, $v_c = 50, 80, 100$ m/min
Coolant	Emulsion

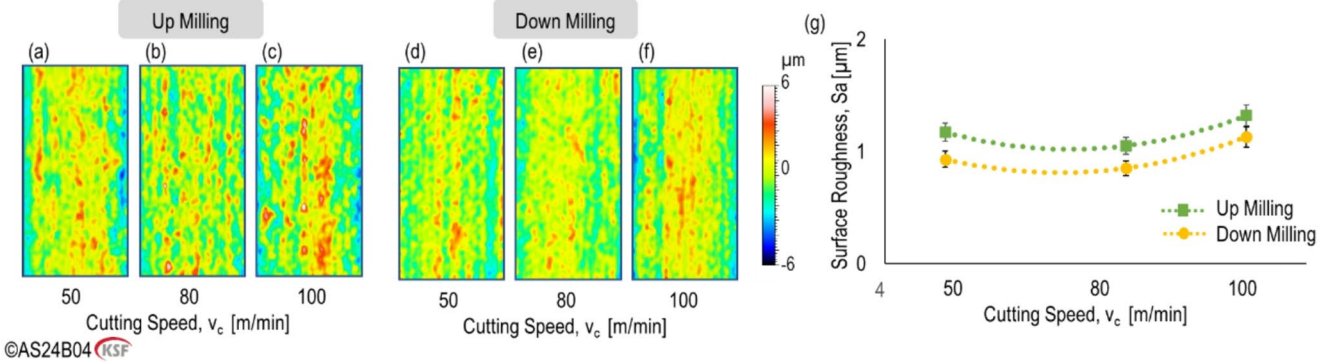
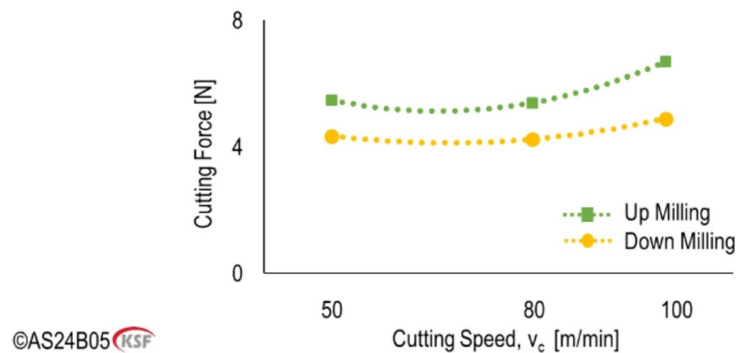


Fig. 4 Confocal microscopy images of micro side-milled surfaces at cutting speeds of 50, 80, and 100 m/min: (a–c) up-milling and (d–f) down-milling conditions. (g) Surface roughness parameter (Sa) corresponding to different cutting speeds in micro up- and down-milling

Fig. 5 Cutting forces in various cutting speeds in micro up and down milling

Process	1- Micro trochoidal milling 2- Micro side milling (up and down milling)
Tool	Ceramic-coated carbide micro milling tool, Ø 0.8 mm, 2 and 4 cutting edges
Workpiece	Hardened steel (AISI D2), hardness = 60HRC
Parameters	Trochoidal milling: $a_e = 0.025$ mm, $a_p = 1$ mm, $f_z = 6$ $\mu\text{m/tooth}$, $v_c = 40$ m/min Side milling: $a_e = 0.01$ mm, $a_p = 1$ mm, $f_z = 6$ $\mu\text{m/tooth}$, $v_c = 50, 80, 100$ m/min
Coolant	Emulsion



Among the tested conditions, the optimal surface quality in down milling occurs at $v_c = 80$ m/min, with Sa value of $0.85 \mu\text{m}$. At a lower cutting speed of 50 m/min, surface quality is only slightly worse, with an 8% increase in Sa, suggesting stable cutting dynamics in this range. However, at $v_c = 100$ m/min, surface quality deteriorates significantly, with a 32% increase in Sa compared to 80 m/min. This reduction is attributed to increased thermal and runout effects, which destabilize the cutting process and introduce surface irregularities.

The superior performance of down milling over up milling can be explained by the direction of chip formation and material flow. In down milling, the cutting forces push the tool into the material, minimizing deflection and achieving

smoother surfaces. In contrast, up milling involves forces that lift the tool, increasing deflection and leading to a rougher surface.

This trend is also evident in the force measurements presented in Fig. 5, which illustrates the cutting forces at different cutting speeds and milling strategies. The cutting force behavior closely follows the trend observed in surface roughness. At cutting speeds of 50 m/min and 80 m/min, the cutting forces in both up and down milling remain nearly identical, with minimal differences. However, at 100 m/min, a noticeable increase in cutting force is observed. The cutting forces diagram in Fig. 5 reflect the underlying chip formation mechanisms that govern both surface integrity and burr evolution. Under stable conditions at 50 m/min

and 80 m/min, the nearly identical force profiles indicate a steady shearing action with uniform chip segmentation and limited lateral material flow, which explains the smoother surfaces obtained in these regimes. However, the force increase observed at higher cutting speeds signifies intensified thermal–mechanical interaction at the tool–workpiece interface, promoting partial ploughing and material adhesion along the edge.

3.2.2 Burr formation

Figure 6(a, b) presents microscopy images of burrs formed after micro-milling and histograms depicting average burr height and width for various f_z values in up micro milling. The results indicate that the smallest burr dimensions are achieved at $f_z = 4$ and $6 \mu\text{m}/\text{tooth}$, with burr heights of $1.57 \mu\text{m}$ and widths of about $9 \mu\text{m}$, respectively. Increasing f_z to $8 \mu\text{m}/\text{tooth}$ leads to a rise in burr dimensions, with average burr height reaching $5 \mu\text{m}$ and average width increasing to $15 \mu\text{m}$. This increase is attributed to higher material removal rates, resulting in greater cutting forces and uncontrolled material flow along the edges. Similarly, at $f_z = 2 \mu\text{m}/\text{tooth}$, burr height and width are larger than at 4 and $6 \mu\text{m}/\text{tooth}$. This is due to the tool’s cutting-edge radius exceeding the feed per tooth, causing ploughing instead of shearing, increasing material deformation, and leading to excessive burr formation.

Figure 7(a, b) presents optical microscopy images of burr formation at the edges of milled surfaces under different cutting speeds and milling strategies (up and down milling), along with the corresponding average burr height and width. At v_c of 80 m/min, the smallest burr dimensions are observed: $1.3 \mu\text{m}$ in average height and $7.5 \mu\text{m}$ in average

width for down milling, compared to $1.57 \mu\text{m}$ and $8.5 \mu\text{m}$, respectively, for up milling. Across all cutting speeds, down milling consistently yields better results than up milling, producing smaller burrs due to reduced tool deflection and controlled material flow.

While the difference in burr height between 50 and 80 m/min is minimal, average burr height increase at v_c of 100 m/min, particularly in up milling. This trend is evident in the microscopy images, where the burrs at v_c of 100 m/min in up milling are larger, indicating unstable cutting conditions including higher cutting temperature, more plastic deformation and tool deflection. Similarly, burr width follows this pattern: the difference between up and down milling is smallest at 80 m/min, while at 50 and 100 m/min, the variations become more pronounced, showing increased instability and material deformation at suboptimal speeds.

The optimal parameter set for micro side milling of hardened steel, which provides the best surface quality and the lowest burr dimensions, consists f_z of $6 \mu\text{m}$, v_c of 80 m/min, and down milling as the preferred strategy.

3.2.3 Deburring

Figure 8 shows the microscopic images (400X magnification) of the edges of the milled surfaces after top polishing using a polyurethane-bonded SiC polishing pin ($\Phi 1 \text{ mm}$) at different axial depths of cuts. Achieving burr-free but sharp edges (without edge rounding) after milling is critical in many industries to ensure functionality, precision, and quality. The deburring and polishing process, as indicated in Fig. 1(b), was performed directly in the CNC machine.

As seen in Fig. 8, using an a_p of 0.05 mm effectively removes all burrs from the edges, leaving the surface clean

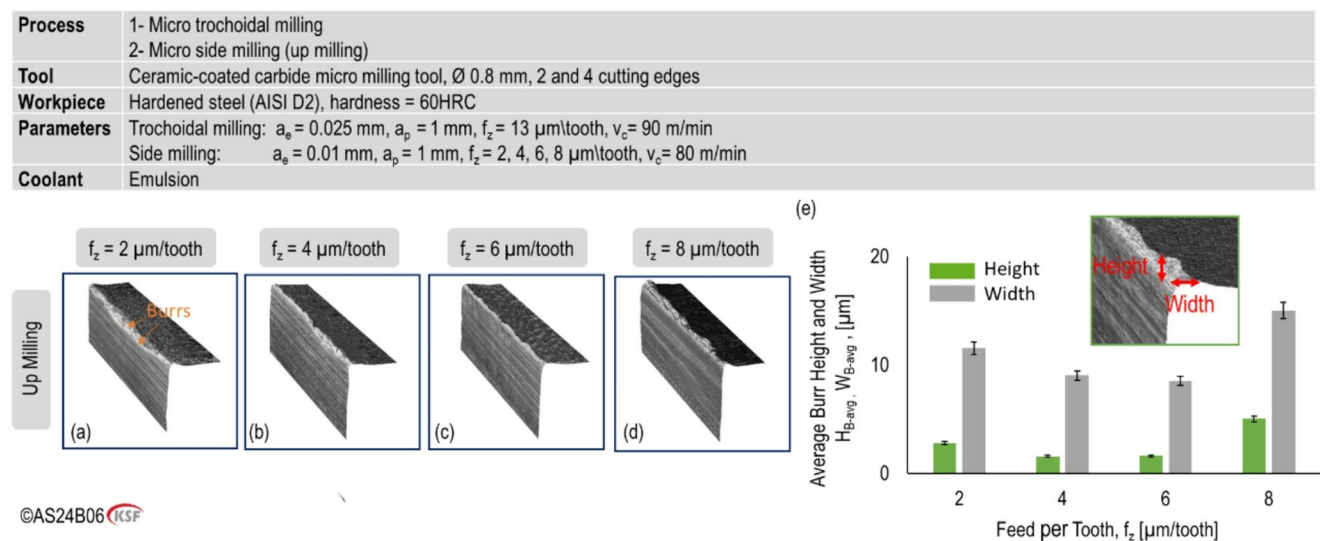
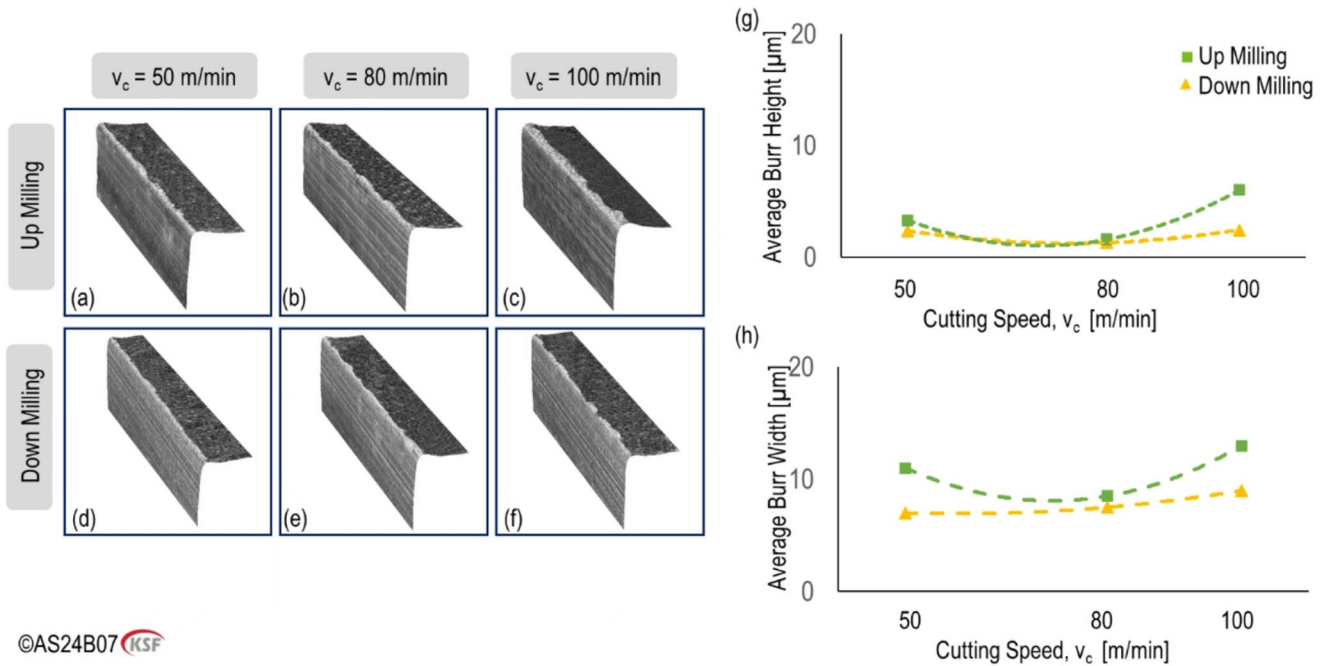


Fig. 6 Microscopic images of burr formation in micro-milling at different feed per tooth values of 2, 4, 6, and $8 \mu\text{m}/\text{tooth}$: (a–d). (e) Average burr height and width corresponding to various feeds per tooth in micro-milling

Process	1- Micro trochoidal milling 2- Micro side milling (up and down milling)
Tool	Ceramic-coated carbide micro milling tool, \varnothing 0.8 mm, 2 and 4 cutting edges
Workpiece	Hardened steel (AISI D2), hardness = 60HRC
Parameters	Trochoidal milling: $a_e = 0.025$ mm, $a_p = 1$ mm, $f_z = 13$ $\mu\text{m}/\text{tooth}$, $v_c = 90$ m/min Side milling: $a_e = 0.01$ mm, $a_p = 1$ mm, $f_z = 6$ $\mu\text{m}/\text{tooth}$, $v_c = 50, 80, 100$ m/min
Coolant	Emulsion

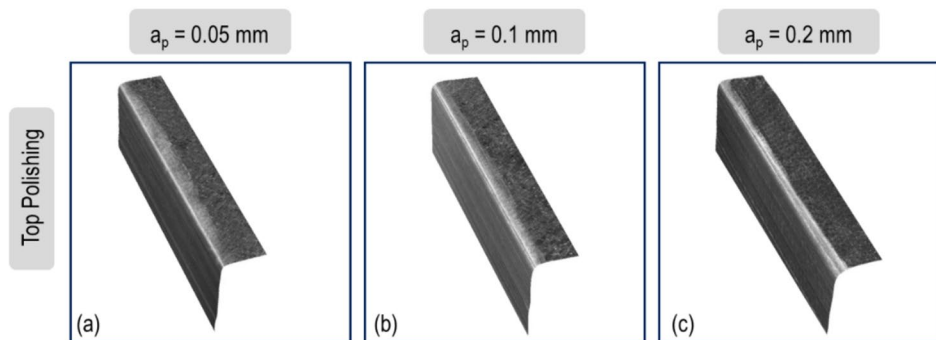


©AS24B07 (KSF)

Fig. 7 Microscopic images of burrs formed after micro-milling at different cutting speeds of 50, 80, and 100 m/min: (a–c) up-milling and (d–f) down-milling. (g) Average burr height and (h) average burr width corresponding to various cutting speeds in micro up- and down-milling

Fig. 8 microscopy images of the edges of milled slots after deburring using different axial depths of cut (a) 0.05 mm, (b) 0.01 mm and (c) 0.2 mm in micro-top polishing

Process	1- Micro trochoidal milling 2- Micro side milling (down milling) 3- Micro polishing (top polishing)
Tool	Ceramic-coated carbide micro milling tool, \varnothing 0.8 mm, 2 and 4 Cutting Edges, Polyurethane-bonded SiC polishing pin (Φ 1 mm)
Workpiece	Hardened steel (AISI D2), hardness = 60HRC
Parameters	Trochoidal milling: $a_e = 0.025$ mm, $a_p = 1$ mm, $f_z = 13$ $\mu\text{m}/\text{tooth}$, $v_c = 90$ m/min Side milling: $a_e = 0.01$ mm, $a_p = 1$ mm, $f_z = 6$ $\mu\text{m}/\text{tooth}$, $v_c = 80$ m/min Top polishing: $a_e = 0.25$ mm, $a_p = 0.05, 0.1, 0.2$ mm, $v_{ft} = 100$ mm/min, $v_c = 50$ m/min
Coolant	Emulsion



©AS24B08 (KSF)

and well-defined without any visible deterioration and edge rounding. The polishing action is more controlled, focusing on burr removal without excessive abrasion. However, increasing the a_p to 0.1 mm results in slight rounding of the edges, indicating the onset of edge deterioration of the workpiece. At an a_p of 0.2 mm, the edges exhibit significant deterioration, characterized by excessive rounding and a complete loss of sharp definition.

The deterioration observed at higher a_p values can be attributed to increased contact pressure and aggressive material removal, which over-polishes the edges and damages their geometry.

To provide a quantitative assessment of these effects, the average edge rounding radii were measured as 30 μm , 54 μm , and 66 μm for polishing depths of 0.05 mm, 0.1 mm, and 0.2 mm, respectively. These results confirm that higher axial polishing depths intensify edge rounding due to greater tool–workpiece contact and abrasive interaction. The polishing depth of 0.05 mm therefore represents the optimal condition, achieving complete burr removal while maintaining sharp, well-defined edges and minimizing dimensional alteration of the slot geometry.

A comparison with other reported micro-deburring methods further highlights the efficiency of the proposed CNC-based post-polishing process. For instance, Kumar et al. [26] investigated ultrasonic-assisted abrasive micro-deburring, where complete burr removal required approximately 10 s for soft materials such as aluminum and copper, and 3–6 min for hard-to-cut materials including Ti-6Al-4 V and bearing steel. In contrast, the present method achieves complete deburring of hardened steel (60 HRC) within a few seconds per edge directly inside the CNC machining center, without the need for external ultrasonic or fluidic systems. The removal mechanism in this study is based on controlled mechanical micro-abrasion using a polyurethane-bonded SiC polishing tool, which preserves edge geometry and ensures high surface uniformity. This integrated approach therefore offers significant advantages in process automation, geometric accuracy, and cycle-time reduction compared with existing hybrid or ultrasonic-assisted techniques.

4 Conclusion

This study addressed challenges in the micro-milling of hardened steel, specifically AISI D2 with hardness of 60 HRC, focusing on minimizing burr formation and enhancing surface quality. Initial slots were machined using trochoidal micro-milling strategy, followed by an evaluation of micro-finishing parameters to determine the optimal conditions for achieving superior surface quality and minimal burr dimensions. Additionally, an innovative CNC deburring method

was introduced, integrating polyurethane-bonded SiC polishing tools within a CNC machining center immediately after milling, resulting in burr-free micro slots. The key findings of this study are summarized below.

- Trochoidal milling with a_p of 0.1 mm was identified as the most efficient roughing strategy, providing an optimal balance between machining time and surface quality. Although lower a_p value (e.g., 0.025 mm) resulted in improved surface finish, it significantly increased machining time, making the process less practice.

al for efficient manufacturing.

- The best surface quality ($S_a=0.85 \mu\text{m}$) and minimal burr dimensions (average burr height=1.3 μm , average burr width=7.5 μm) were achieved at v_c of 80 m/min, f_z of 6 μm , and down micro milling. Deviations from these parameters, whether lower or higher feed per tooth and cutting speeds, led to deteriorated surface quality and increased burr formation due to alterations in cutting mechanics and process instability.
- Down milling consistently produced better results than up milling across all cutting speeds, resulting smoother surfaces and smaller burrs due to reduced tool deflection and improved material flow. Moderate feed per tooth of 4–6 μm minimized burr height and width, while lower (2 $\mu\text{m}/\text{tooth}$) or higher feed rates (8 $\mu\text{m}/\text{tooth}$) resulted in larger burrs due to ploughing effects or process instability.
- A polyurethane-bonded SiC polishing tool with a_p of 0.05 mm effectively removed burrs without causing edge deterioration. However, increasing a_p to 0.1–0.2 mm led to edge rounding and damage.

The integration of deburring within the CNC machining process improved process consistency, minimized manual intervention, and ensured high-quality edge finishes, facilitating sustainable production in automotive, aerospace, and medical industries.

4.1 Future work

Future work will focus on extending the proposed CNC-based post-polishing approach to other difficult-to-machine materials such as titanium alloys and stainless steels to evaluate its general applicability. Further investigations will include optimization of polishing tool geometry, grit size, and process parameters to reduce cycle time while maintaining edge sharpness. In addition, the integration of real-time monitoring and feedback control for burr detection and adaptive polishing will be explored to develop a fully automated and intelligent deburring system suitable for high-precision micro-manufacturing environments.

Acknowledgements Special thanks also to GF Machining Solutions for providing the Mikron MILL S 400 U[®] 5-axis milling machine, and EVE Ernst Vetter for their participation in the Automated Micro Polishing (AMP) project.

Authors' contributions The conception of the study was undertaken by Bahman Azarhoushang. Material preparation, data collection, and analysis were performed by Armin Siahsharani, and Masih Paknejad. The first draft of the manuscript was written by Armin Siahsharani, with Bahman Azarhoushang reviewing and editing version. All authors read and approved the final manuscript.

Funding Open Access funding enabled and organized by Projekt DEAL. This work is funded by Zentrales Innovationsprogramm Mittelstand (ZIM) (Grant KK 5110602KT1).

Data availability Not applicable.

Code availability Not applicable.

Declarations

Ethics approval Not applicable.

Consent to participate Not applicable.

Consent for publication Not applicable.

Conflicts of interest/Competing interests Not applicable.

Open Access This article is licensed under a Creative Commons Attribution 4.0 International License, which permits use, sharing, adaptation, distribution and reproduction in any medium or format, as long as you give appropriate credit to the original author(s) and the source, provide a link to the Creative Commons licence, and indicate if changes were made. The images or other third party material in this article are included in the article's Creative Commons licence, unless indicated otherwise in a credit line to the material. If material is not included in the article's Creative Commons licence and your intended use is not permitted by statutory regulation or exceeds the permitted use, you will need to obtain permission directly from the copyright holder. To view a copy of this licence, visit <http://creativecommons.org/licenses/by/4.0/>.

References

- O'Toole L, Kang C-W, Fang F-Z (2021) Precision micro-milling process: state of the art. *Adv Manuf* 9:173–205
- Luo X, Cheng K, Webb D, Wardle F (2005) Design of ultraprecision machine tools with applications to manufacture of miniature and micro components. *J Mater Process Technol*. <https://doi.org/10.1016/j.jmatprotec.2005.05.050>
- Rosli AM, Jamaludin AS, Razali MNM (2021) Recent study on hard to machine material–micromilling process
- Saedon J, Soo S, Aspinwall D, Barnacle A (2012) Micro-milling of hardened AISI D2 tool steel. *Adv Mater Res* 445:62–67
- Cui X, Zhao J (2014) Cutting performance of coated carbide tools in high-speed face milling of AISI H13 hardened steel. *Int J Adv Manuf Technol* 71:1811–1824
- Mallick R, Kumar R, Panda A, Sahoo AK (2020) Performance characteristics of hardened AISI D2 steel turning: a review. *Mater Today Proc* 26:2685–2690
- Balázs B, Takács M (2020) Experimental investigation and optimisation of the micro milling process of hardened hot-work tool steel. *Int J Adv Manuf Technol* 106(11):5289–5305
- Balázs BZ, Geier N, Pereszlai C, Poór DI, Takács M (2021) Analysis of cutting force and vibration at micro-milling of a hardened steel. *Procedia CIRP* 99:177–182
- Hojati F, Baraheni M, Azarhoushang B (2024) Research on ploughing to shearing transition in micro milling of titanium alloy using Gramian angular field and machine learning methods. *Arab J Sci Eng*, pp. 1–13
- Wu X-J, Tong X (2018) Study of trajectory and experiment on steel polishing with elastic polishing wheel device. *Int J Adv Manuf Technol* 97(1):199–208
- Balázs B, Takács M (2020) A comparative analysis of characteristics of cutting forces at micro-milling of hardened steels, in *IOP Conference Series: Materials Science and Engineering*, vol. 903, no. 1: IOP Publishing, p. 012056
- Oliaei SNB, Karpat Y (2014) Experimental investigations on micro milling of stavax stainless steel. *Procedia CIRP* 14:377–382
- Siahsharani A, Bayat M, Alinaghizadeh A, Azarhoushang B, Böisinger R, Amini S (2025) Surface integrity optimization in milling of aluminum 1100: effects of supercritical CO₂+ MQL and emulsion cooling with various milling strategies. *Int J Adv Manuf Technol*, pp. 1–14
- Niu Z, Jiao F, Cheng K (2018) An innovative investigation on chip formation mechanisms in micro-milling using natural diamond and tungsten carbide tools. *J Manuf Process* 31:382–394
- Silva LC, da Silva MB (2019) Investigation of burr formation and tool wear in micromilling operation of duplex stainless steel. *Precis Eng* 60:178–188
- Sun Q, Cheng X, Zhao G, Yang X, Zheng G (2019) Experimental study of micromilling burrs of 304 stainless steel. *Int J Adv Manuf Technol* 105:4651–4662
- Gomes MC, da Silva MB, Duarte MAV (2020) Experimental study of micromilling operation of stainless steel. *Int J Adv Manuf Technol* 111:3123–3139
- Xie Y, Chang G, Yang J, Zhao M, Li J (2022) Process optimization of robotic polishing for mold steel based on response surface method. *Machines* 10(4):283
- Xiao G, Huang Y, Yin J (2017) An integrated polishing method for compressor blade surfaces. *Int J Adv Manuf Technol* 88(5):1723–1733
- Cho S-S, Ryu Y-K, Lee S-Y (2002) Curved surface finishing with flexible abrasive tool. *Int J Mach Tools Manuf* 42(2):229–236
- Brinksmeier E, Riemer O, Gessenharter A (2006) Finishing of structured surfaces by abrasive polishing. *Precis Eng* 30(3):325–336
- Hajiahmadi S (2019) Burr size investigation in micro milling of stainless steel 316L. *Int J Lightweight Mater Manuf* 2(4):296–304
- Siahsharani A, Alinaghizadeh A, Azarhoushang B, Bayat M, Böisinger R (2025) Sustainable and efficient cooling in titanium milling for dental applications: a study on supercritical CO₂+MQL with focus on tool wear and surface topography. *Wear* 572:206051
- dos Santos AJ, de Oliveira DA, Pereira NFS, Abrão AM, Rubio JCC, Câmara MA (2024) Effect of conventional and trochoidal milling paths on burr formation during micromilling of grade 4 commercially pure titanium. *Arab J Sci Eng* 49(2):1727–1742
- Shixiong W, Wei M, Bin L, Chengyong W (2016) Trochoidal machining for the high-speed milling of pockets. *J Mater Process Technol* 233:29–43
- Kumar AS, Deb S, Paul S (2021) Ultrasonic-assisted abrasive micro-deburring of micromachined metallic alloys. *J Manuf Process* 66:595–607

Publisher's note Springer Nature remains neutral with regard to jurisdictional claims in published maps and institutional affiliations.